International Global Navigation Satellite Systems Society
IGNSS Symposium 2009

Holiday Inn Surfers Paradise, Qld, Australia
1 – 3 December, 2009

On the Time-To-Fix for Single-Frequency GNSS-Based Attitude Determination

G. Giorgi
Delft Institute of Earth Observation and Space Systems,
Delft University of Technology, The Netherlands
+31 152782713 G.Giorgi@tudelft.nl

P.J.G. Teunissen
Department of Spatial Sciences,
Curtin University of Technology, Perth, Australia
+61 892667676 p.teunissen@curtin.edu.au

ABSTRACT

The GNSS-based Attitude Determination is a demanding application which requires a precise relative positioning solution. In order to obtain an accurate estimate of a platform's orientation, a GNSS receiver must fix the integer ambiguities inherent to the phase observables: the ambiguity resolution process is the key for exploiting the higher precision of carrier phase measurements with respect to the code measurements. Among the set of admissible integer ambiguity estimators, we focus on the optimal Integer Least-Squares estimator, which has been modified to include a geometrical non-linear constraint on the baseline length that arises when considering two antennae separated by a known distance. The challenge of reliable and fast integer estimation is particularly hard for single-frequency applications: the method proposed in this contribution leads to a strong reduction on the Time-To-Fix, i.e. the number of epochs needed to achieve a sufficient reliability on the fixed ambiguity vector. Simulation and experimental results showed the large improvement obtained when applying the non-linear constrained model.

KEYWORDS: Attitude, GNSS, LAMBDA, ILS, TTF

1. INTRODUCTION

GNSS-based Attitude Determination is a challenging high precise relative navigation application. In order to fully exploit the precision of the GNSS measurements, the phase observations must be employed, which are of two orders of magnitude more accurate than the code observations. The phase measurements are however affected by integer ambiguities, which must be resolved: the fixing process is challenging especially if one aims at fast (ideally single-epoch) and single-frequency solutions.
The problem of ambiguity resolution for Attitude Determination is a rich area of study, and many techniques have been developed to cope with the issue, see e.g. Bar-Itzhack *et al.* (1997), Cohen (1992), Han and Rizos (1999), Kim and Langley (2000), Lu (1995), Park *et al.* (1996), Tu *et al.* (1996), Crassidis *et al.* (1997), Ziebart and Cross (2003).

In this work we concentrate on the LAMBDA (Least squares AMBiguity Decorrelation Adjustment) method. This algorithm, introduced in Teunissen (1993, 1994, 1995), is a fast, reliable and widely used implementation of the ILS (Integer Least-Squares) estimator, which was shown to be optimal in Teunissen (1999).
When the baseline length is known, the components of the baseline vector must fulfill a non-linear geometrical constraint: this leads to a modification of the ILS problem to a constrained ILS problem. To solve for the nonlinear constrained model, an extension of the original LAMBDA method is needed, as addressed in Teunissen (2006, 2008, 2008b). The introduction of the constraint on the baseline length makes the determination of the integer minimizer more difficult, in particular with regard to the search strategies to be adopted to perform the search in a large set of admissible integer candidates. Two search methods have been developed to cope with such a problem: the *Expansion* and the *Search and Shrink* approaches (Teunissen, 2006; Buist, 2007; Giorgi *et al.*, 2008). Both methods provide a fast procedure for the search of the integer minimizer and are described in this contribution. The single-epoch performances of the new method are reported, and the increment in the single-epoch/single-frequency success rate is demonstrated.
An important aspect of the constrained ILS is the capacity of reducing the number of epochs needed to achieve a certain probability of fixing the correct integer vector of ambiguities: this is extensively studied through simulations and a kinematic test, and the large reduction with respect to the unconstrained ILS is shown.

2. THE FUNCTIONAL AND STOCHASTIC MODELS FOR THE GNSS OBSERVABLES

In this section the functional and stochastic models for the GNSS phase and code observables are introduced. It is shown how the geometrical constraint on the baseline length is included in a model solvable in the framework of the Integer Least-Squares theory.

Assuming two antennae simultaneously tracking *n+1* satellites on a single-frequency, any linearized double difference set of GNSS observations at a given epoch can be described via a Gauss-Markov model:

$$\begin{aligned} E(y) &= Aa + Bb \quad a \in \mathbb{Z}^n \; ; \; b \in \mathbb{R}^p \\ D(y) &= Q_{yy} \end{aligned} \tag{1}$$

where *E(y)* is the expectation operator, *y* is the vector of code and phase observables (order *2n*), *a* is the vector of integer ambiguities (order *n*), and *b* is the vector of the *p* real-valued unknowns. Any atmosphere error is neglected, limiting the analysis to short baselines; it is assumed that the only real-valued unknowns are the three baseline coordinates, so that *p = 3*. *A* is the *2n×n* matrix containing the carrier wavelengths while *B* is the *2n×3* matrix containing the unit line-of-sight vectors. The second line of (1) describes the stochastic model: *D(y)* is the dispersion operator and Q_{yy} is the *2n×2n* variance-covariance (v-c) matrix of the observables. If the baseline length is assumed to be constant, a quadratic constraint ($||b||^2 = l^2$) is added to the model (1):

$$\begin{aligned} E(y) &= Aa + Bb \quad a \in \mathbb{Z}^n \; ; \; b \in \mathbb{R}^3 \; ; \; \|b\| = l \\ D(y) &= Q_{yy} \end{aligned} \tag{2}$$

The solution of this model must indeed respect two constraints: the integerness of the ambiguities and the geometrical constraint on the baseline vector. Constraining the baseline length has a straightforward geometrical interpretation: it is equivalent to impose the extremity of the vector b to lie on the surface of a sphere of radius *l*.

When the observations span *k* epochs, the models (1)-(2) are rewritten as

$$E\begin{pmatrix} y_1 \\ y_2 \\ \vdots \\ y_k \end{pmatrix} = \begin{bmatrix} A & B_1 & 0 & \cdots & 0 \\ A & 0 & B_2 & \cdots & 0 \\ \vdots & & & \ddots & \\ A & 0 & 0 & \cdots & B_k \end{bmatrix} \begin{pmatrix} a \\ b_1 \\ b_2 \\ \vdots \\ b_k \end{pmatrix} = M_k \begin{pmatrix} a \\ b_1 \\ b_2 \\ \vdots \\ b_k \end{pmatrix} \qquad (3)$$

$$D\begin{pmatrix} y_1 \\ y_2 \\ \vdots \\ y_k \end{pmatrix} = \begin{bmatrix} Q_{yy} & 0 & \cdots & 0 \\ 0 & Q_{yy} & \cdots & 0 \\ & & \ddots & \\ 0 & 0 & \cdots & Q_{yy} \end{bmatrix} = I_k \otimes Q_{yy}$$

where the symbol $\otimes$ denotes the Kronecker product. The ambiguities must be integers, $a \in \mathbb{Z}^n$, and for the constrained model the set of *k* non-linear geometrical constraints has to be considered: $\|b_i\| = l$; $i = 1,\ldots,k$. It is assumed that the baseline length does not vary during the *k* epochs considered.

Every epoch is considered independent from the others in the stochastic model (a correlation could be easily considered) and the v-c matrix of the observations is taken constant over the time span. The model (3) holds true as long as neither carrier cycle slips nor a change in the number of tracked satellites occur.

3. INTEGER LEAST-SQUARES

In this section the solutions of the unconstrained and constrained models are presented, together with two strategies developed to make the search for the integer minimizer more efficient.

3.1 The unconstrained solution

The Least-Squares solution of the unconstrained model (1) was coined an ILS problem due to the integer nature of the ambiguities. The ILS estimator is demonstrated to be optimal among the class of admissible integer estimators (Teunissen, 1999), meaning that the ILS has the (statistical) property of maximizing the probability of estimating the correct integer values for the ambiguities. The solution of (1) is derived following a three-step procedure. Firstly, a float solution is obtained disregarding the integerness of the ambiguities, by solving the set of normal equations

$$N \cdot \begin{pmatrix} \hat{a} \\ \hat{b} \end{pmatrix} = \begin{bmatrix} A & B \end{bmatrix}^T Q_{yy}^{-1} y \qquad \text{with} \qquad N = \begin{bmatrix} A & B \end{bmatrix}^T Q_{yy}^{-1} \begin{bmatrix} A & B \end{bmatrix} \qquad (4)$$

The variance-covariance matrices of the float solutions are

$$\begin{bmatrix} Q_{\hat{a}\hat{a}} & Q_{\hat{a}\hat{b}} \\ Q_{\hat{b}\hat{a}} & Q_{\hat{b}\hat{b}} \end{bmatrix} = N^{-1} \qquad (5)$$

Aiming to minimize the squared norm of the residuals of (1), it is useful to consider the following sum-of-squares decomposition:

$$\|y - Aa - Bb\|^2_{Q_{yy}} = \|\hat{e}\|^2_{Q_{yy}} + \|\hat{a} - a\|^2_{Q_{\hat{a}\hat{a}}} + \left\|\hat{b}(a) - b\right\|^2_{Q_{\hat{b}(a)}} \qquad (6)$$

where $\|\cdot\|^2_Q = (\cdot)^T Q^{-1}(\cdot)$, $\hat{e}$ is the vector of least-squares residuals and $\hat{b}(a)$ is the conditional

baseline solution, i.e. the corrected float solution assuming the vector of ambiguities known:

$$\hat{b}(a) = \hat{b} - Q_{\hat{b}\hat{a}} Q_{\hat{a}\hat{a}}^{-1} (\hat{a} - a) \tag{7}$$

$Q_{\hat{b}(a)}$ is the corresponding v-c matrix:

$$Q_{\hat{b}(a)} = Q_{\hat{b}\hat{b}} - Q_{\hat{b}\hat{a}} Q_{\hat{a}\hat{a}}^{-1} Q_{\hat{a}\hat{b}} \tag{8}$$

It is clear that, not imposing any constraint on *b*, the last term of (6) can be made zero for any integer-valued vector *a*, and the minimizer of (6) is

$$\breve{a} = \arg\min_{a \in \mathbb{Z}^n} \left\| \hat{a} - a \right\|_{Q_{\hat{a}\hat{a}}}^2 \tag{9}$$

The sought for vector of integer ambiguities has the closest distance with respect to the float solution in the metric of the v-c matrix $Q_{\hat{a}\hat{a}}$. Since no analytical solutions of (9) are known, an extensive search in a subset of the *n*-dimensional space of integers is necessary.

The LAMBDA method is a well-known and reliable implementation of the ILS estimator. It works by first decorrelating the original v-c matrix of ambiguities $Q_{\hat{a}\hat{a}}$, via an admissible transformation (i.e. which preserves the integerness of the variables in both the direct and the inverse transformations) (Teunissen, 1998); then the integer minimizer (9) is extensively searched inside the set (see Figure 1)

$$\Omega^U\left(\chi^2\right) = \left\{ a \in \mathbb{Z}^n \,|\, \left\| \hat{a} - a \right\|_{Q_{\hat{a}\hat{a}}}^2 \le \chi^2 \right\} \tag{10}$$

Geometrically, $\Omega^U\left(\chi^2\right)$ describes an hyper-ellipsoid centred at $\hat{a}$ with size and shape governed by the entries of $Q_{\hat{a}\hat{a}}$: the effect of the decorrelation is to strongly reduce the elongation of such hyper-ellipsoid, so that the search is performed in a more efficient and, most important, faster way.

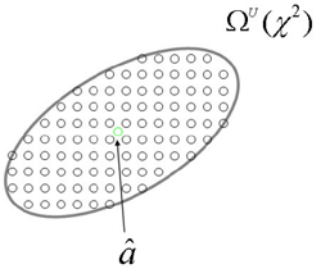

Figure 1. The ellipsoidal search space $\Omega^U\left(\chi^2\right)$

The scalar χ^2 has to be chosen carefully: it needs to be small enough to limit the computational burden, but the non-emptiness of $\Omega^U\left(\chi^2\right)$ should be guaranteed. A good choice is to make use of the bootstrapped value a_b (Teunissen, 2006b) to set the size of Ω^U:

$$\chi^2 = \left\| \hat{a} - a_b \right\|_{Q_{\hat{a}\hat{a}}}^2 \tag{11}$$

Once the integer minimizer $\breve{a}$ is found, the baseline vector is given by equation (7): as the expression (8) states, the precision of the fixed baseline solution is improved with respect to the float solution.

3.2 The constrained solution

When the baseline vector *b* has to fulfill the non-linear geometrical constraint, generally the last term on the right-hand side of (6) cannot be made zero for any choice of the vector of ambiguities *a*. The solution of the constrained model (2) is addressed in Teunissen (2006, 2008, 2008b), where the proposed implementation of the constrained ILS is coined the Constrained LAMBDA algorithm.

The minimization problem is modified as

$$\breve{a} = \arg\min_{a \in \mathbb{Z}^n} \left(\| \hat{a} - a \|_{Q_{\hat{a}\hat{a}}}^2 + \| \hat{b}(a) - \breve{b}(a) \|_{Q_{\hat{b}(a)}}^2 \right) = \arg\min_{a \in \mathbb{Z}^n} F(a) \tag{12}$$

with

$$\breve{b}(a) = \arg \min_{b \in \mathbb{R}^3,\ \|b\|=l} \| \hat{b}(a) - b \|^2_{Q_{\hat{b}(a)}} \tag{13}$$

where the sought for integer vector $\breve{a}$ not only weighs the distance from the float solution $\hat{a}$ (in the metric of $Q_{\hat{a}\hat{a}}$), but also the distance of the baseline solution $\hat{b}(a)$ (given the ambiguity vector) to the sphere with radius equal to the known baseline length, weighted by the v-c matrix $Q_{\hat{b}(a)}$. Geometrically, the constrained least-squares problem (13) consists in projecting the conditional baseline solution $\hat{b}(a)$ on the surface of a sphere of radius *l*, in the metric of the v-c matrix $Q_{\hat{b}(a)}$. Equivalently, (13) could be seen as the problem of finding the point of contact between the sphere of radius *l* and the three-dimensional ellipsoid centred in $\hat{b}(a)$ and shape governed by $Q_{\hat{b}(a)}$.

In principle the search for the minimizer of (12) can be performed extensively, as the unconstrained ILS, by means of searching inside the set

$$\Omega^C\left(\chi^2\right) = \{a \in \mathbb{Z}^n \mid F(a) \le \chi^2\} \tag{14}$$

The weight matrix of the baseline term makes the search trickier than the unconstrained case: since the entries of the matrix $Q_{\hat{b}(a)}$ are driven by the precise phase observations, the second term in (12) has a higher weight than the first. This has two consequences: firstly, the search space where the integer-valued vector *a* is searched is no longer ellipsoidal as it was for $\Omega^U\left(\chi^2\right)$. Secondly, the choice for the scalar χ^2 becomes very critical: setting its value by picking up an integer vector a' and computing

$$\chi^2 = F(a') \tag{15}$$

generally leads to unacceptable large values for χ^2, for which the computational burden is too high. The reason for this lies in the fact that the higher weight of the second term largely amplifies the values of χ^2 for any non-correct value of *a*. Moreover, the evaluation of the modified cost function involves the solution of a non-linear minimization problem, hence increasing the computational time associated to the evaluation of the residuals for each ambiguity vector.

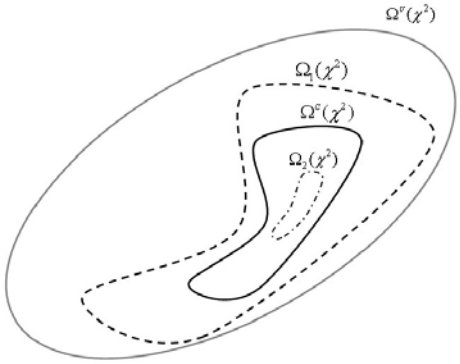

Figure 2. The relation between the search spaces $\Omega^C\left(\chi^2\right)$, $\Omega^U\left(\chi^2\right)$ and the two bounding sets $\Omega_1\left(\chi^2\right)$ and $\Omega_2\left(\chi^2\right)$, for a given scalar χ

Two approaches were proposed to overcome these issues: the search strategies were coined the *Expansion* and the *Search and Shrink* approaches (Park and Teunissen, 2003; Buist, 2007; Giorgi *et al.*, 2008).

The cost function $F(a)$ is bounded via the following two inequalities:

$$F_1(a) \le F(a) \le F_2(a)$$

$$F_1(a) = \| \hat{a} - a \|^2_{Q_{\hat{a}\hat{a}}} + \lambda_m \left(\| \hat{b}(a) \| - l \right)^2 \tag{16}$$

$$F_2(a) = \| \hat{a} - a \|^2_{Q_{\hat{a}\hat{a}}} + \lambda_M \left(\| \hat{b}(a) \| - l \right)^2$$

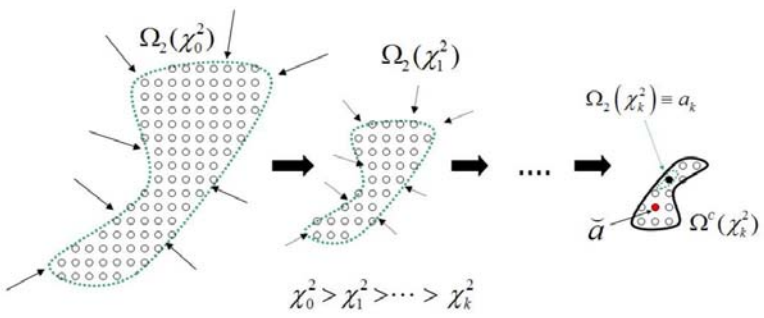

Figure 3. *Search and Shrink* approach

where λ_m and λ_M are the smallest and the largest eigenvalues of the matrix $Q_{\hat{b}(a)}^{-1}$. The term $\left(\|\hat{b}(a)\| - l\right)$ is the distance between $\hat{b}(a)$ and the sphere of radius l, and it coincides with the value that the second term of the cost function $F(a)$ would assume if the weight matrix $Q_{\hat{b}(a)}^{-1}$ were a unit matrix. The aim of the introduction of $F_1(a)$ and $F_2(a)$ is to work with functions that are easier to evaluate than the original $F(a)$, for which the solution of a non-linear constrained problem (13) has to be found.

We define two search spaces associated to the two bounding functions as

$$\begin{aligned} \Omega_1\left(\chi^2\right) &= \{a \in \mathbb{Z}^n \,|\, F_1(a) \le \chi^2\} \\ \Omega_2\left(\chi^2\right) &= \{a \in \mathbb{Z}^n \,|\, F_2(a) \le \chi^2\} \\ \Omega_2\left(\chi^2\right) \subseteq \Omega^C\left(\chi^2\right) &\subseteq \Omega_1\left(\chi^2\right) \subseteq \Omega^U\left(\chi^2\right) \end{aligned} \tag{17}$$

where the last relationship follows from the inequalities (16), and it is represented in Figure 2.

The first proposed method is the *Search and Shrink* approach, visualized in Figure 3. This approach was introduced in Teunissen (2008) and tested in Giorgi *et al.* (2008). Initially, a proper integer vector is used to set the value of χ_0^2 to guarantee the non-emptiness of $\Omega_2\left(\chi_0^2\right)$. Then, a search is performed to find an integer vector in $\Omega_2\left(\chi_0^2\right)$, say a_1, for which the value χ^2 can be made smaller: $\chi_1^2 = F_2(a_1) < F_2(a_0) = \chi_0^2$. As soon as such vector is found, the scalar χ^2, and so the associated set $\Omega_2\left(\chi^2\right)$, is shrunk to a reduced size. The search proceeds by iteratively shrinking the search space until only one integer vector lies inside the set, say a_k. Because of the inequalities (16), the found integer vector, which minimizes $F_2(a)$, might or might not be also the minimizer of $F(a)$. For this reason, setting $\chi_k^2 = F_2(a_k)$, all the integer vectors in $\Omega^C\left(\chi_k^2\right)$ are evaluated and the minimizer of $F(a)$ is extracted.

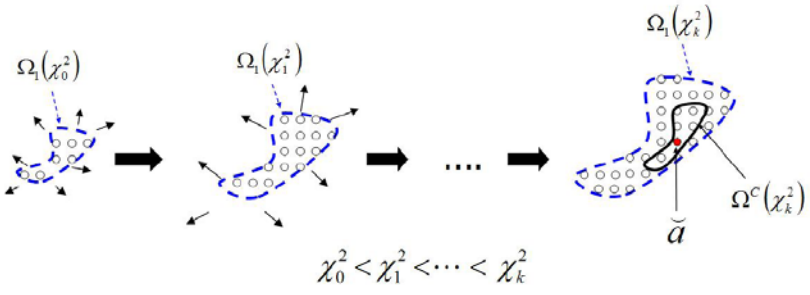

Figure 4. *Expansion* approach

The second proposed search method is the *Expansion* approach (see Park and Teunissen, 2003; Buist, 2007), illustrated in Figure 4. Firstly, all the integer vectors contained in the set $\Omega_1\left(\chi_0^2\right)$, with χ_0 chosen small enough, are enumerated and each one is used to compute the

problem (13). Hence, the set $\Omega^C\left(\chi_0^2\right)$ is evaluated: if it is empty, the scalar χ is increased ($\chi_1 > \chi_0$), otherwise the minimizer of (12) is extracted. The main advantage of this method is that the search begins in a small search space, and the computation of a least-squares problem is limited to a very small set of candidates. By iteratively increasing the value of χ^2, the method quickly converges towards a non-empty set $\Omega^C\left(\chi^2\right)$, without the need for evaluating the problem (13) a large number of times.

The use of the *Expansion* and the *Search and Shrink* approaches, which have proved to work equally well, makes the search for the integer minimizer (12) much faster, compared to the extensive search.

3.3 The multi-epoch solution

Considering a time window of *k* epochs, both the unconstrained and constrained methods presented can be extended to solve for the model (3). The main benefit of having a multi-epoch processing is the higher accuracy of the float solution, and therefore an increased probability of fixing the correct integer vector.
We begin to derive the float solutions $\hat{a}$ and $\hat{b}_i$ from the set of normal equations

$$N \cdot \begin{pmatrix} \hat{a}_k \\ \hat{b}_1 \\ \vdots \\ \hat{b}_k \end{pmatrix} = M_k^T \left(I_k \otimes Q_{yy}^{-1}\right) y \qquad \text{with} \qquad N = M_k^T \left(I_k \otimes Q_{yy}^{-1}\right) M_k \tag{18}$$

The v-c matrices of the float solutions are

$$\begin{bmatrix} Q_{\hat{a}_k\hat{a}_k} & Q_{\hat{a}_k\underline{\hat{b}}} \\ Q_{\underline{\hat{b}}\hat{a}_k} & Q_{\underline{\hat{b}}\underline{\hat{b}}} \end{bmatrix} = N^{-1} \tag{19}$$

Where $\hat{a}_k$ indicates the ambiguity float solution when *k*-epochs are processed. $Q_{\underline{\hat{b}}\underline{\hat{b}}}$ is the ($3k \times 3k$) v-c matrix for the different values assumed by the baseline vector *b* during the $i = 1, \ldots, k$ epochs processed:

$$Q_{\underline{\hat{b}}\underline{\hat{b}}} = \begin{bmatrix} Q_{\hat{b}_1\hat{b}_1} & Q_{\hat{b}_1\hat{b}_2} & \cdots & Q_{\hat{b}_1\hat{b}_k} \\ Q_{\hat{b}_2\hat{b}_1} & Q_{\hat{b}_2\hat{b}_2} & \cdots & Q_{\hat{b}_2\hat{b}_k} \\ & & \ddots & \\ Q_{\hat{b}_k\hat{b}_1} & Q_{\hat{b}_k\hat{b}_2} & \cdots & Q_{\hat{b}_k\hat{b}_k} \end{bmatrix} \quad ; \quad Q_{\hat{a}_k\underline{\hat{b}}} = \begin{bmatrix} Q_{\hat{a}_k\hat{b}_1} & Q_{\hat{a}_k\hat{b}_2} & \cdots & Q_{\hat{a}_k\hat{b}_k} \end{bmatrix} = Q_{\underline{\hat{b}}\hat{a}_k}^T \tag{20}$$

The float solution could be obtained recursively assuming a motion model for the baseline. However, in this contribution only a batch processing strategy is analysed: the reason for this is that an optimal solution for the minimizer of a multi-epoch constrained model cannot be obtained recursively in a rigorous manner (Teunissen, 2007).
The baseline solutions, provided the vector of ambiguities known, are

$$\begin{pmatrix} \hat{b}_1(a) \\ \hat{b}_2(a) \\ \vdots \\ \hat{b}_k(a) \end{pmatrix} = \begin{pmatrix} \hat{b}_1 \\ \hat{b}_2 \\ \vdots \\ \hat{b}_k \end{pmatrix} - Q_{\underline{\hat{b}}\hat{a}_k} Q_{\hat{a}_k\hat{a}_k}^{-1} (\hat{a}_k - a) \tag{21}$$

with v-c matrix

$$Q_{\underline{\hat{b}}(a)} = Q_{\underline{\hat{b}}\underline{\hat{b}}} - Q_{\underline{\hat{b}}\hat{a}_k} Q^{-1}_{\hat{a}_k\hat{a}_k} Q_{\hat{a}_k\underline{\hat{b}}} \tag{22}$$

Because of the shape of the M_k and Q_y matrices, the v-c matrix $Q_{\underline{\hat{b}}(a)}$ has a block diagonal structure:

$$Q_{\underline{\hat{b}}(a)} = \begin{bmatrix} \left(B_1^T Q_{yy}^{-1} B_1\right)^{-1} & & \cdots & 0 \\ 0 & \left(B_2^T Q_{yy}^{-1} B_2\right)^{-1} & \cdots & 0 \\ \vdots & & \ddots & \\ 0 & & \cdots & \left(B_k^T Q_{yy}^{-1} B_k\right)^{-1} \end{bmatrix} = \begin{bmatrix} Q_{\hat{b}_1(a)} & & \cdots & 0 \\ 0 & Q_{\hat{b}_2(a)} & \cdots & 0 \\ \vdots & & \ddots & \\ 0 & & \cdots & Q_{\hat{b}_k(a)} \end{bmatrix} \tag{23}$$

This is a consequence of the assumption made on the absence of correlation between epochs: each of the conditional baseline vector is uncorrelated with all the others.
The sum-of-square decomposition of the squared norm of residual of (3) is

$$\left\| \begin{matrix} y_1 - B_1 b_1 - Aa \\ \vdots \\ y_k - B_k b_k - Aa \end{matrix} \right\|^2_{I_k \otimes Q_{yy}} = \sum_{i=1}^{k} \| e_i \|^2_{Q_{yy}} + \left\| \hat{a}_k - a \right\|^2_{Q_{\hat{a}\hat{a}}} + \sum_{i=1}^{k} \| \hat{b}_i(a) - b_i \|^2_{Q_{\hat{b}_i(a)}} \tag{24}$$

When no constraint on the baseline length is assumed, the last term can be made zero for any ambiguity vector, and the integer minimizer is found by minimizing the second term via the unconstrained LAMBDA method. The entries of the matrix $Q_{\hat{a}_k\hat{a}_k}$ are reduced with respect to the single-epoch case, and therefore the probability of fixing the correct integer vector increases.
For the constrained case, the epoch-by-epoch baseline solutions must respect the constraint on the length: from the sum-of-squares decomposition (24) follows that the function to be minimized is

$$\breve{a} = \arg\min_{a \in \mathbb{Z}^n} \left(\| \hat{a}_k - a \|^2_{Q_{\hat{a}_k\hat{a}_k}} + \sum_{i=1}^{k} \| \hat{b}_i(a) - \breve{b}_i(a) \|^2_{Q_{\hat{b}_i(a)}} \right) = \arg\min_{a \in \mathbb{Z}^n} F(a) \tag{25}$$

with

$$\breve{b}_i(a) = \arg \min_{b_i \in \mathbb{R}^3, \|b_i\| = l} \| \hat{b}_i(a) - b_i \|^2_{Q_{\hat{b}_i(a)}} \tag{26}$$

The search for the minimizer $\breve{a}$ can proceed as the single-epoch case depicted in the previous section, with the substitution of the original bounding functions with

$$\begin{aligned} F_1(a) \le F(a) \le F_2(a) \\ F_1(a) = \| \hat{a}_k - a \|^2_{Q_{\hat{a}_k\hat{a}_k}} + \sum_{i=1}^{k} \lambda_m^i \left(\| \hat{b}_i(a) \| - l \right)^2 \\ F_2(a) = \| \hat{a}_k - a \|^2_{Q_{\hat{a}_k\hat{a}_k}} + \sum_{i=1}^{k} \lambda_M^i \left(\| \hat{b}_i(a) \| - l \right)^2 \end{aligned} \tag{27}$$

where λ_m^i and λ_M^i are the smallest and the largest eigenvalues of the matrix $Q^{-1}_{\hat{b}_i(a)}$.

4. SIMULATIONS RESULTS

The proposed implementation for the constrained LAMBDA was been initially tested with

simulated data, to check the performance in a controlled environment, with a known set of error sources. In this section the simulation set-up is explained and we present the outcomes.

4.1 Simulation set up

Date and time	22 Jan 2008 00:00
Location	Lat: 50° , Long:3°
GPS week	439
Frequency	L1
Number of Satellites (PRNs)	PDOP
5 (8,10,15,26,28)	4.192
6 (8,10,15,26,28,18)	2.142
7 (8,10,15,26,28,18,9)	1.917
8 (8,10,15,26,28,18,9,21)	1.811
Undifferenced code noise σ_p $[cm]$	30 - 15 - 5
Undifferenced phase noise σ_ϕ $[mm]$	30 - 3 - 1
Baseline length	2m
Samples simulated	10^5

Table 1. Simulation set up.

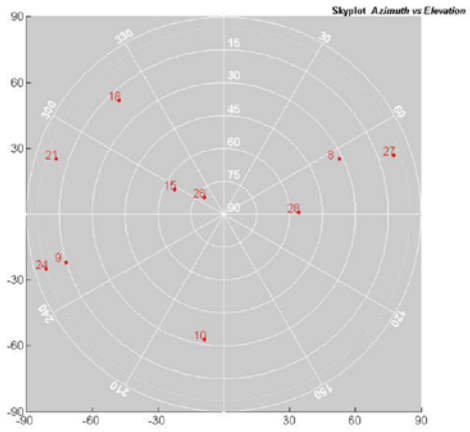

Figure 5. Skyplot of the GPS constellation as seen from 50° latitude North,3° Longitude East, on 22 Jan 2008

The simulation inputs are summarized in Table 1: based on the geometry of the actual GPS constellation on 22 January 2008 (see Figure 5), we simulated 10^5 samples of data for a set of scenarios, which differ for undifferenced code (30-15-5 cm) and phase (30-3-1 mm) noise levels, and number of satellites (from 5 to 8). We considered a 2m length static baseline; no multipath effect was introduced in the simulated observations. The 36 sets were processed with both the unconstrained LAMBDA and the constrained LAMBDA. Two aspects of the proposed methods were carefully investigated: the increment in success rate, defined as the percentage of epochs where the vector of integer ambiguities is correctly resolved, and the number of epochs to be processed in order to achieve a pre-determined probability of fixing the correct integer vector.

4.2 Simulation outcomes

Firstly the single-frequency/single-epoch success rate of the unconstrained and constrained LAMBDA was analysed on the different simulated scenarios.
Table 2 summarizes the outcomes for the two methods: the improvement achieved with the constrained LAMBDA is clear. As expected, the strengthening of the underlying model strongly affected the capacity of fixing the correct integer ambiguity vector, in particular for the weaker scenarios (lower number of satellites / higher noise levels), where the difference

σ_ϕ $[mm]$		30			3			1		
σ_p $[cm]$		30	15	5	30	15	5	30	15	5
# satellites	*Method*	*Single-epoch/single-frequency success rate*								
5	U	0.5	3.2	29.8	3.50	20.0	86.2	6.40	28.4	95.3
	C	3.6	9.6	42.0	73.7	86.4	**99.5**	95.8	**100**	**100**
6	U	0.6	4.3	32.4	23.3	67.4	96.8	51.3	87.0	**100**
	C	3.3	11.4	44.1	96.6	**99.6**	**99.9**	**100**	**100**	**100**
7	U	0.9	3.5	32.8	49.9	80.4	**99.4**	75.3	92.9	**100**
	C	6.6	13.1	45.1	**99.4**	**99.9**	**100**	**100**	**100**	**100**
8	U	2.0	5.7	36.6	86.0	93.9	**100**	**99.7**	**100**	**100**
	C	8.3	16.8	47.4	**99.7**	**100**	**100**	**100**	**100**	**100**

Table 2. Simulation results: single-frequency, single-epoch success rates for the unconstrained (U) and constrained (C) LAMBDA methods. Success rates higher than 99% are highlighted.

σ_ϕ [mm]		30			3			1		
σ_p [cm]		30	15	5	30	15	5	30	15	5
# satellites	*Method*	*# epochs needed to achieve 99% success rate*								
5	U	> 30	> 30	8	> 30	14	3	> 30	13	2
	C	> 30	29	7	4	3	1	2	1	1
6	U	> 30	> 30	7	12	4	2	9	3	1
	C	> 30	26	6	2	1	1	1	1	1
7	U	> 30	19	5	9	3	1	6	2	1
	C	26	13	4	1	1	1	1	1	1
8	U	25	12	5	3	2	1	2	1	1
	C	14	8	4	1	1	1	1	1	1

Table 3. Simulation results: number of epochs needed to guarantee a single-frequency success rate higher than 99% over 10^5 data simulated. U: unconstrained LAMBDA method ; C: constrained LAMBDA method

between the methods was large. It can be noted for example that the scenario characterized by 1mm phase noise and 30cm code noise exceptionally improved from 6% to almost 96% of successfully fixed ambiguities.
Table 2 also shows that for sufficiently strong scenarios (higher number of satellites/lower noise levels) the difference between the two methods was small, and the unconstrained LAMBDA already provided good results. In particular a significant dependence on the code noise was observed: the lower the value, the smaller the improvement that one can obtain passing from the unconstrained to the constrained method. This is due to the weighting of the two terms of the cost function (12): the matrices $Q_{\hat{a}\hat{a}}$ and $Q_{\hat{b}(a)}$ are driven by the code and phase noise values, respectively. When the difference between the two noise levels decreases, the relative weight associated to the baseline term reduces with respect to the ambiguity term, and so does the difference of the success rates achieved.

The second aspect investigated was the Time-To-Fix, defined here as the number of epochs needed to assure a certain (experimental) probability of success rate. Each of the simulated scenarios was solved on a multi-epoch base, varying the *k* number of epochs used.
Table 3 reports, for each of the scenarios, the number of epochs needed in the batch processing to achieve a success rate of at least 99%. As expected, the constrained LAMBDA assured a strong reduction of the number of epochs to be employed, in particular for some of the weaker scenarios. Like the single-epoch case, the difference between the unconstrained and the constrained solutions was reduced when the noise on the code data was made smaller.

Tables 2 and 3 show that a large improvement in performance was obtained when using the constrained LAMBDA method. Firstly, the single-epoch/single-frequency processing provided striking results, confirming that a single-epoch solution is feasible when strengthening the underlying model. The outcomes relative to the scenarios with 3mm undifferenced phase noise, which are of higher practical relevance, show that the constrained method provided success rates higher than 99% on most of the set, whereas the unconstrained model achieved the same result only in two cases. As for the multi-epoch results, the same set of scenarios needed at most only 4 epochs to guarantee success rates higher than 99%, and it always required less epochs than the unconstrained case.
We remark that the inclusion of the scenarios characterized by a 30mm noise on the undifferenced phase observations is too pessimistic, but it is useful to investigate the limits of the proposed algorithm.

5. TESTING THE METHOD: A VESSEL COMPASS SOLUTION

5.1 The kinematic test set up

Figure 6. A picture of the ship used for the kinematic experiment.
1: choke-ring antenna connected to the Ashtech reciver
2: antenna connected to the Leica SR530 receiver
3: antenna connected to the Novatel OEM3 receiver

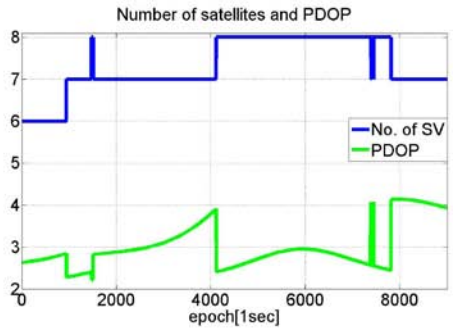

Figure 7. Number of tracked satellites and PDOP during the vessel experiment

The algorithm was tested on data collected on board a ship sailing on the Schie river, Delft, The Netherlands. The vessel was sailed up and down the river for about 2.5 hours, collecting 9000 epochs of single-frequency GPS observations from different antennae. We tested the algorithm on the 2m long baseline formed by the antennae 1-2 and the 1.5m long baseline formed by the antennae 2-3 (see Figure 6). The receivers employed were an Ashtech Z-12, a Leica SR530 and a Novatel OEM3. Figure 7 reports the number of satellites tracked and the PDOP values for the duration of the test.

5.2 Experimental results

The collected observations were processed with both the unconstrained and constrained methods: Table 4 reports the single-epoch and multi-epoch/single-frequency success rates obtained.
As shown, the constrained LAMBDA method was capable to provide single-epoch/single-frequency success rates higher than 97% on both the baselines considered, whereas the unconstrained model did not provide fixing rates higher than 82%. In particular, the improvement on the baseline 2-3 was rather large, passing from 62% for the unconstrained method to 97% for the constrained algorithm.
It is noteworthy that applying the constrained LAMBDA on the baseline 1-2, the single-epoch solution was sufficient to get a 99% of success rate (with 7 epochs a 100% success rate was reached), and only a 3-epochs window was needed to obtain the same result on the baseline 2-3. The unconstrained LAMBDA showed lower performance, due to the weaker model; the multi-epoch processing provided a certain improvement, but not to the same extent as the constrained method. In particular, we could not get 100% of success rate even considering 50-epochs of data.
To better highlight the benefits of exploiting the constraint, Table 5 reports the single-epoch

		Baseline 1-2		Baseline 2-3	
	k	*LAMBDA*	*constrained LAMBDA*	*LAMBDA*	*constrained LAMBDA*
Single-epoch success rate (%)	1	82.01	99.59	61.73	97.70
Multi-epoch success rate (%)	2	84.10	99.88	68.19	98.52
	5	85.40	99.92	73.81	99.12
	10	85.82	100	77.49	99.40
	20	86.36	100	81.22	99.61

Table 4. Vessel experiment results: single-epoch and multi-epoch success rate

		Baseline 1-2		Baseline 2-3	
# satellites	*Method*	*Single-epoch*	*10-epochs*	*Single-epoch*	*10-epochs*
6	U	28.33	25.69	8.81	22.67
	C	97.78	100	84.58	93.49
7	U	81.15	87.45	54.70	74.36
	C	99.75	100	98.73	99.98
8	U	96.67	98.95	83.46	94.94
	C	99.97	100	99.84	100

Table 5. Vessel experiment results: single-epoch and 10-epochs success rate (%) as function of number of satellites tracked, for the unconstrained (U) and constrained (C) LAMBDA methods

and 10-epochs success rates as function of the number of satellites tracked. The performance of the constrained model was higher especially for observations collected when less satellites were available.
Figures 8-9 show the single-epoch Compass solution (in terms of Heading and Elevation angles) for the two baselines, obtained respectively with the unconstrained and the constrained LAMBDA algorithms.
Figures 10-11 report the Compass solution for the 10-epochs processing: it is evident the reduction of the number of uncorrected fixed ambiguities, which results in less scattered plots.

6. CONCLUSIONS

The problem of resolving the integer ambiguities which affect the GNSS phase carrier observations is the key for precise relative positioning solution. The theory of Integer Least Squares is widely used to fix the ambiguities, and the LAMBDA method is a fast and reliable mechanized procedure to implement the ILS. When two antennae are kept to a fixed and known distance, a non-linear constraint can be embedded in the theory, to the purpose of strengthening the model and improving the capacity of fixing the correct ambiguity vector. The non-linear constrained ILS principle was studied, and the constrained LAMBDA method was proposed as an implementation. Two approaches (the *Expansion* and the *Search and Shrink*) were described to efficiently perform the search for the integer minimizer.

The proposed method was firstly tested on a set of simulated data, investigating the influence of the number of available satellites and the noise levels on the code and phase observations: the difference between the unconstrained and the constrained LAMBDA was generally large, with large improvements in success rate for the weaker scenarios.
An important aspect of the constrained model is the reduction of the Time-To-Fix: through simulations it was shown how the constrained method can effectively reduce the time needed to reliably fix the vector of integer ambiguities.
The algorithm was then tested on data collected on a vessel, for which the Compass solution was derived. The constrained LAMBDA outperformed the unconstrained method, allowing to correctly fix the ambiguities for more than 97% of the time already with the single-epoch/single-frequency solution. Only few epochs (namely 3) are necessary to obtain more than 99% of success rate for the multi-epoch model on both the baselines processed.

The application of the new method to both simulated and experimental data showed that the inclusion of the non-linear geometrical constraint provides a large improvement, making the ambiguity fixing process more reliable and effectively reducing the Time-To-Fix.

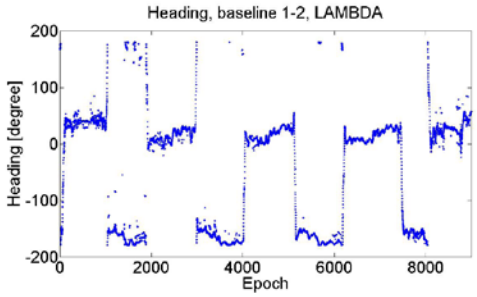

(a) Heading angle, baseline 1-2

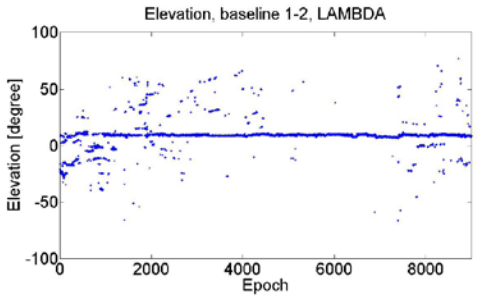

(b) Elevation angle, baseline 1-2

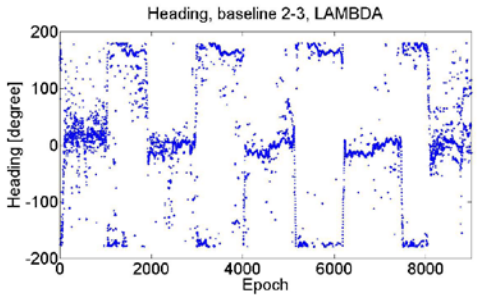

(c) Heading angle, baseline 2-3

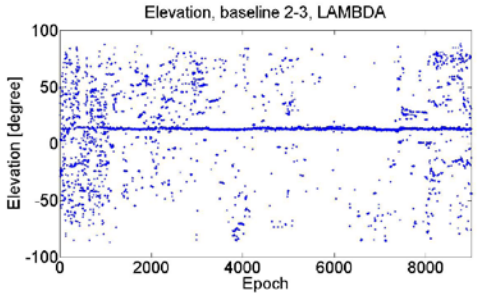

(d) Elevation angle, baseline 2-3

Figure 8. Single-epoch/single-frequency compass solution for the baselines 1-2 and 2-3, LAMBDA method

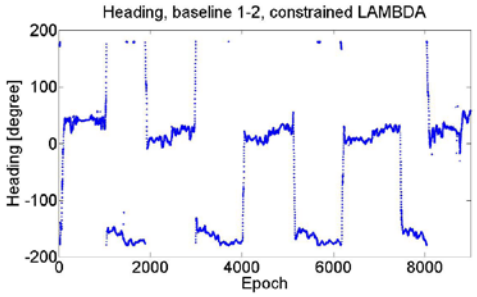

(a) Heading angle, baseline 1-2

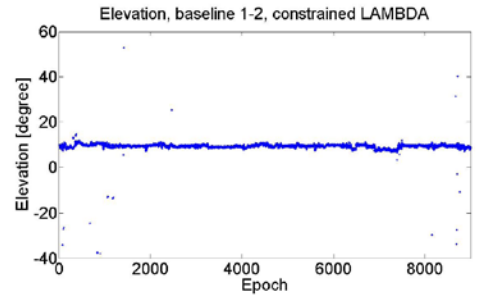

(b) Elevation angle, baseline 1-2

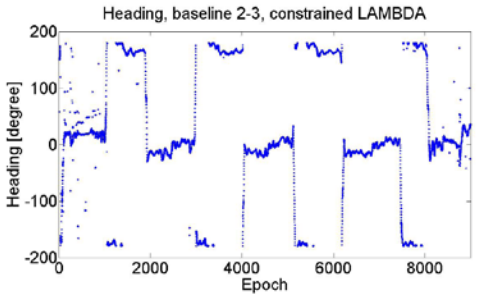

(c) Heading angle, baseline 2-3

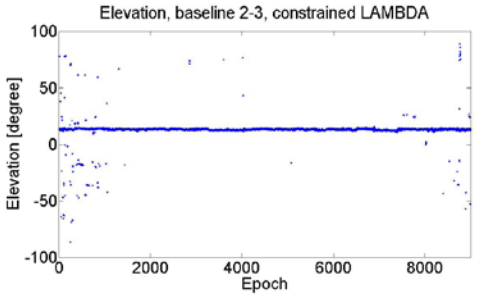

(d) Elevation angle, baseline 2-3

Figure 9. Single-epoch/single-frequency compass solution for the baselines 1-2 and 2-3, constrained LAMBDA method

ACKNOWLEDGEMENTS

Professor P.J.G. Teunissen is the recipient of an Australian Research Council Federation Fellowship (project number FF0883188). This support is greatly acknowledged.
Dr. S. Verhagen is acknowledged for the fruitful comments provided; Ir. P. Buist is also acknowledged for the precious comments.

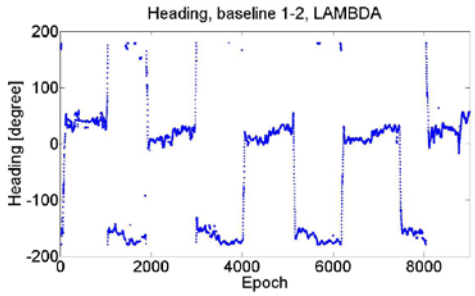

(a) Heading angle, baseline 1-2

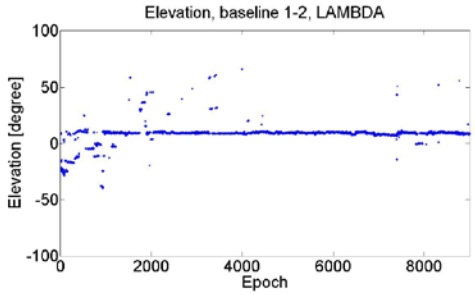

(b) Elevation angle, baseline 1-2

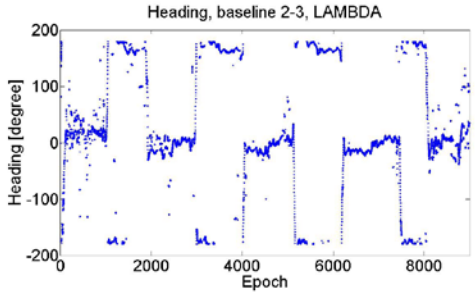

(c) Heading angle, baseline 2-3

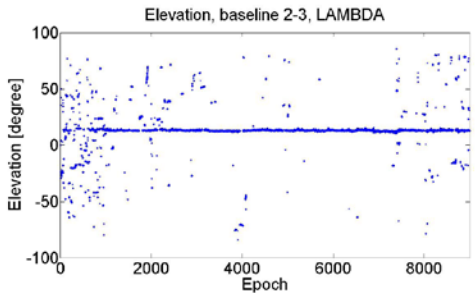

(d) Elevation angle, baseline 2-3

Figure 10. 10-epochs/single-frequency compass solution for the baselines 1-2 and 2-3, LAMBDA method

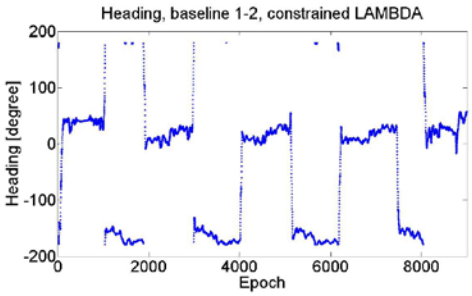

(a) Heading angle, baseline 1-2

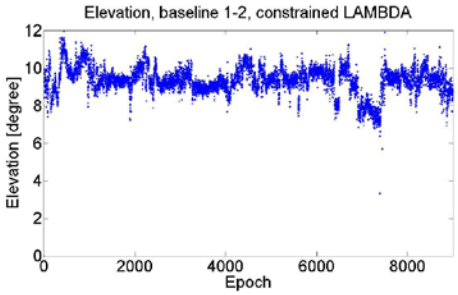

(b) Elevation angle, baseline 1-2

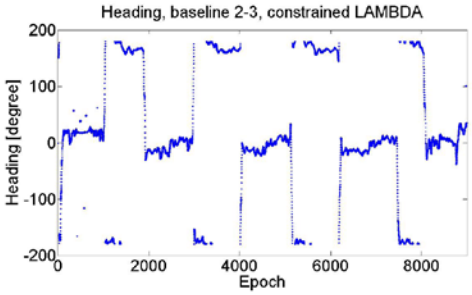

(c) Heading angle, baseline 2-3

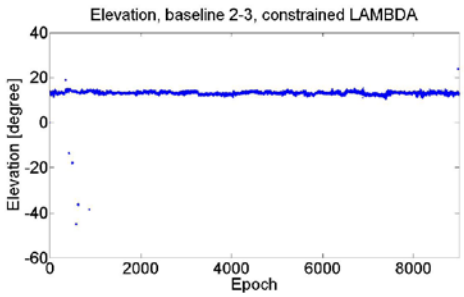

(d) Elevation angle, baseline 2-3

Figure 11. 10-epochs/single-frequency compass solution for the baselines 1-2 and 2-3, constrained LAMBDA method

REFERENCES

Bar-Itzhack IY, Montgomery P, Garrick J (1997) Algorithm for Attitude Determination using GPS, *Proceedings of AIAA Guidance, Navigation and Control Conference*, New Orleans, LA, USA, Paper no.AIAA 97- 3616.

Buist PJ (2007) The Baseline Constrained LAMBDA Method for Single Epoch, Single Frequency Attitude Determination Applications, *Proceedings of ION-GPS*, Forth Worth, Texas, USA.

Cohen CE (1992) Attitude Determination Using GPS, *PhD Thesis*.

Crassidis JL, Markley FL, Lightsey EG (1997) A New Algorithm for Attitude Determination Using Global Positioning System Signals, *AIAA Journal of Guidance, Control, and Dynamics*, 20(5):891-896.

Giorgi G, Teunissen PJG, Buist PJ (2008) A Search and Shrink Approach for the Baseline Constrained LAMBDA: Experimental Results, *Proceedings of the International Symposium on GPS/GNSS*, Tokyo, Japan.

Han S, Rizos C (1999) Single-Epoch Ambiguity Resolution for Real-Time GPS Attitude Determination with the Aid of One-Dimensional Optical Fiber Gyro, *GPS Solutions*, 3:5-12.

Kim D, Langley RB (2000) GPS ambiguity resolution and validation: Methodologies, trends and issues, *Presented at the 7th GNSS Workshop – International Symposium on GPS/GNSS*, Seoul, Korea.

Lu G (1995) Development of a GPS Multi-antenna System for Attitude Determination, *UCGE Reports 20073*, Dept. of Geomatics Eng., University of Calgary.

Park C, Kim I, Lee JG, Jee GI (1996) Efficient Ambiguity Resolution Using Constraint Equation, *Proceedings of IEEE: Position, Location and Navigation Symposium PLANS96*, Atlanta, Georgia, USA.

Park C, Teunissen PJG (2003) A New Carrier Phase Ambiguity Estimation for GNSS Attitude Determination Systems, *Proceedings of the International Symposium on GPS/GNSS*, Tokyo, Japan.

Teunissen PJG (1993) Least Squares Estimation of the Integer GPS Ambiguities, *Invited lecture, Section IV Theory and Methodology*, IAG General Meeting, Beijing.

Teunissen PJG (1994) A New Method for Fast Carrier Phase Ambiguity Estimation, *Proceedings IEEE Position Location and Navigation Symposium, PLANS '94*, 562–573.

Teunissen PJG (1995) The Least-Squares Ambiguity Decorrelation Adjustment: a Method for Fast GPS Integer Ambiguity Estimation, *Journal of Geodesy*, Springer, 70:65–82.

Teunissen PJG, Kleusberg A (1998) *GPS for Geodesy*, Springer, Berlin Heidelberg New York.

Teunissen PJG (1999) An Optimality Property of the Integer Least-Squares Estimator, *Journal of Geodesy*, Springer, 73(11):587–593.

Teunissen PJG (2006) The LAMBDA Method for the GNSS Compass, *Artificial Satellites*, Vol.41,N.3.

Teunissen PJG (2006b) Influence of Ambiguity Precision on the Success Rate of GNSS Integer Ambiguity Bootstrapping, *Journal of Geodesy*, Springer, 81(5):351–358.

Teunissen PJG (2007) A General Multivariate Formulation of the Multi-Antenna GNSS Attitude Determination Problem, *Artificial Satellites*, Vol.42,N.2.

Teunissen PJG (2008) GNSS Ambiguity Resolution for Attitude Determination: Theory and Method, *Proceedings of the International Symposium on GPS/GNSS*, Tokyo, Japan.

Teunissen PJG (2008b) Integer Least Squares Theory for the GNSS Compass, *Journal of Geodesy*, Springer, *submitted*.

Tu CH, Wang KY, Melton WC (1996) GPS Compass: A Novel Navigation Equipment, *Proceedings of ION National Technical Meeting*, Santa Monica, CA, USA

Ziebart M, Cross P (2003) LEO GPS Attitude Determination Algorithm for a Macro-satellite Using Boomarm Deployed Antennas, *GPS Solutions*, 6:242-256.